

# Controls on tropical Pacific Ocean productivity revealed through nutrient stress diagnostics

Michael J. Behrenfeld<sup>1</sup>, Kirby Worthington<sup>2</sup>, Robert M. Sherrell<sup>3</sup>, Francisco P. Chavez<sup>4</sup>, Peter Strutton<sup>5</sup>, Michael McPhaden<sup>6</sup> & Donald M. Shea<sup>7</sup>

*In situ* enrichment experiments have shown that the growth of bloom-forming diatoms in the major high-nitrate low-chlorophyll (HNLC) regions of the world's oceans is limited by the availability of iron<sup>1–3</sup>. Yet even the largest of these manipulative experiments represents only a small fraction of an ocean basin, and the responses observed are strongly influenced by the proliferation of rare species rather than the growth of naturally dominant populations<sup>4,5</sup>. Here we link unique fluorescence attributes of phytoplankton to specific physiological responses to nutrient stress, and use these relationships to evaluate the factors that constrain phytoplankton growth in the tropical Pacific Ocean on an unprecedented spatial scale. On the basis of fluorescence measurements taken over 12 years, we delineate three major ecophysiological regimes in this region. We find that iron has a key function in regulating phytoplankton growth in both HNLC and oligotrophic waters near the Equator and further south, whereas nitrogen and zooplankton grazing are the primary factors that regulate biomass production in the north. Application of our findings to the interpretation of satellite chlorophyll fields shows that productivity in the tropical Pacific basin may be 1.2–2.5 Pg C yr<sup>-1</sup> lower than previous estimates have suggested, a difference that is comparable to the global change in ocean production that accompanied the largest El Niño to La Niña transition on record<sup>6</sup>.

The tropical Pacific is characterized by warm, well-stratified and nutrient-poor waters separated by a major upwelling plume of nutrient-rich water near the Equator extending from roughly the dateline (180°) to the eastern boundary (Fig. 1a). The upwelled water is rich in dissolved CO<sub>2</sub> that subsequently degasses to the atmosphere. Although the region is the largest natural oceanic source of CO<sub>2</sub> to the atmosphere<sup>7,8</sup>, the extent of this CO<sub>2</sub> release is curtailed to about 0.7–1.5 Pg yr<sup>-1</sup> (1 Pg = 10<sup>15</sup> g) by the photosynthetic carbon uptake of an elevated phytoplankton biomass supported by upwelled macronutrients and micronutrients<sup>8,9</sup>. Throughout the tropical Pacific, variations in physical and chemical properties of the upper ocean imprint resident phytoplankton with physiological characteristics diagnostic of their specific growth constraints. These physiological expressions can be distinguished by associated diel patterns in normalized variable fluorescence ( $F_v/F_m$ )<sup>10</sup>.

We collected more than 140,000 measurements of variable fluorescence along 58,000 km of ship transects during ten field studies between 1994 and 2006 to characterize the broad-scale biological and physiological features of the tropical Pacific (Fig. 1a). Phytoplankton biomass in the study area is distributed similarly to surface nitrate (Fig. 1a), with low values north of roughly 9°N and west of the

dateline, and distinctly elevated values in the equatorial upwelling zone. Daily  $F_v/F_m$  patterns in the tropical Pacific exhibit three dominant features: first, maxima at sunrise and sunset; second, a midday suppression from photoinhibition; and third, a nocturnal decrease (Fig. 1b, c). We find dawn maxima in  $F_v/F_m$  to vary inversely with biomass, having high values in low-nitrate areas and decidedly lower values in upwelling waters (Figs 1b and 2a). Midday photoinhibition

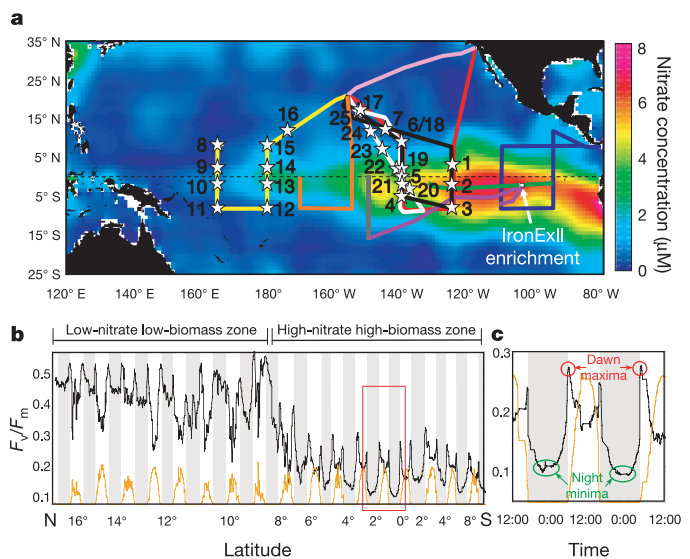


**Figure 1 | The tropical Pacific study area.** **a**, Ship transects (lines) and enrichment experiment locations (stars) for the ten field studies. Transect dates are as follows: grey, 1994; dark purple, 1995; black, 2000; yellow, pink, orange and green, 2001; white, 2002; blue, 2003; red, 2006. The background colour is Levitus climatological surface nitrate concentration, showing elevated values in the equatorial upwelling zone. **b**, Typical variations in normalized variable fluorescence ( $F_v/F_m$ ) for the tropical Pacific, with high dawn values and large photoinhibition in low-nitrate low-biomass regions and low dawn values and large nocturnal decreases in high-nitrate high-biomass areas (data from the 2000 transect, corresponding to the black line in **a** extending from Hawaii to 8°S, 140°W). **c**, Primary diel features in  $F_v/F_m$  (from the red box in **b**) are a nocturnal decrease (circled in green), a dawn maximum (circled in red) and midday photoinhibition. To illustrate the scale of the current investigation, the 64 km<sup>2</sup> IronExII experiment of 1996, which dwarfed earlier bottle enrichments, was only 1/100 the size of the small white rectangle shown in **a** at 2°S, 104°W. The orange lines in **b** and **c** indicate incident sunlight (relative).

<sup>1</sup>Department of Botany and Plant Pathology, Cordley Hall 2082, Oregon State University, Corvallis, Oregon 97331-2902, USA. <sup>2</sup>National Aeronautics and Space Administration, Goddard Space Flight Center, Greenbelt, Maryland 20771, USA. <sup>3</sup>Institute of Marine and Coastal Sciences and Department of Geological Sciences, Rutgers University, 71 Dudley Road, New Brunswick, New Jersey 08901-8521, USA. <sup>4</sup>Monterey Bay Aquarium Research Institute, 7700 Sandholdt Road, Moss Landing, California 95039-9644, USA. <sup>5</sup>College of Oceanic and Atmospheric Sciences, 104 COAS Admin Building, Oregon State University, Corvallis, Oregon 97331-5503, USA. <sup>6</sup>National Oceanic and Atmospheric Administration Pacific Marine Environmental Laboratory, 7600 Sand Point Way NE, Seattle, Washington 98115, USA. <sup>7</sup>Science Applications International Corporation, NASA Goddard Space Flight Center, Greenbelt, Maryland 20771, USA.

is also enhanced in regions of low biomass (Fig. 1b). The remarkable nocturnal decreases in  $F_v/F_m$  are uniform in the upper water column and then disappear in the light-limited lower reaches of the photic zone (see Supplementary Information).

We delineated three physiological regimes in the tropical Pacific on the basis of dawn maxima in  $F_v/F_m$  and the extent of the nocturnal  $F_v/F_m$  decrease (Fig. 2). Regime I is largely found in the north and is characterized by high values (0.45 or more) of  $F_v/F_m$  at dawn and small (less than 25%) nocturnal decreases. Regime II is found west of the upwelling plume and has similarly elevated dawn maxima (Fig. 2a), but exhibits large nocturnal decreases in  $F_v/F_m$  (Fig. 2b). Regime III is distinguished by having chronically low dawn  $F_v/F_m$  and pronounced decreases in  $F_v/F_m$  at night (Fig. 2). The link between these three physiological regimes and specific nutritional constraints was directly tested by conducting 25 small-volume (10-litre) nutrient enrichment experiments (Fig. 1a). These 21–36-h experiments included representatives from all three regimes and involved enrichments of 5  $\mu\text{M}$   $\text{NO}_3$ , 5  $\mu\text{M}$   $\text{NH}_4$ , 1  $\mu\text{M}$   $\text{PO}_4$  and 4 nM iron (see Supplementary Information). Their short duration ensured that observed responses reflected immediate physiological changes rather than growth of the dominant species or a bloom of a rare species.

The addition of  $\text{NO}_3$ ,  $\text{NH}_4$  or  $\text{PO}_4$  had no significant influence on photosynthetic characteristics of samples from regime III. In contrast, addition of iron to samples from regime III consistently eliminated the nocturnal decrease in  $F_v/F_m$ , markedly increased overall  $F_v/F_m$  values to regimes I and II levels (Fig. 3a), enhanced functional absorption cross-sections of oxygen-evolving photosystem II (PSII) complexes and caused a major decrease in electron

turnover times of the plastoquinone (PQ) pool (Fig. 3b, c). In regime II, iron addition similarly removed the nocturnal decrease in  $F_v/F_m$  and generally enhanced electron turnover rates, but dawn  $F_v/F_m$  values were already near maximal and did not change with iron (or  $\text{PO}_4$ ) enrichment (Fig. 3a). Additions of  $\text{NO}_3$  and  $\text{NH}_4$  caused the most striking responses in regime II, inducing marked decreases in  $F_v/F_m$  (Fig. 3a) that were associated with increased background fluorescence levels. Finally, photosynthetic characteristics in regime I remained unaltered after the addition of iron or  $\text{PO}_4$ , and none of the nutrient treatments significantly influenced PSII absorption cross-sections or PQ electron turnover (Fig. 3). The only clear physiological response in regime I was a decrease in  $F_v/F_m$  during four of the eight experiments after  $\text{NO}_3$  or  $\text{NH}_4$  amendment (Fig. 3a). Again, these decreases in  $F_v/F_m$  resulted from an increase in background fluorescence.

Clearly, the three tropical Pacific regimes correspond to different conditions of iron and nitrogen availability. Because many details on the effects of iron stress in plants are known, our population-level fluorescence diagnostics can now be associated with specific phenomena in photosynthetic membranes. Importantly, the photosynthetic apparatus is a major sink for cellular iron, with 24 iron

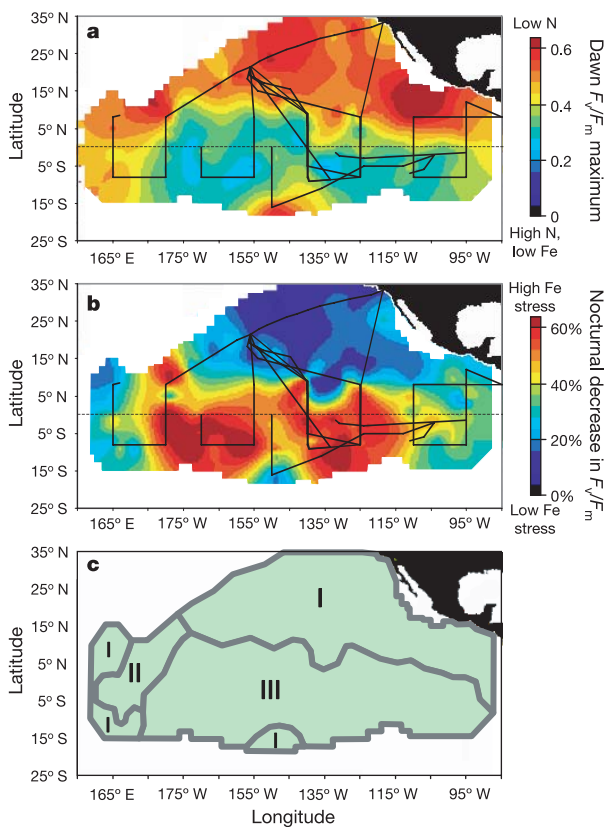


**Figure 2 | Fluorescence diagnostics delineate three physiological regimes in the tropical Pacific.** **a**, Dawn  $F_v/F_m$  maximum. **b**, Nocturnal decrease in  $F_v/F_m$ . **c**, The three regimes: regime I (small nocturnal decreases and high dawn values of  $F_v/F_m$ ), regime II (large nocturnal decreases and high dawn values of  $F_v/F_m$ ) and regime III (large nocturnal decreases and low dawn values of  $F_v/F_m$ ).

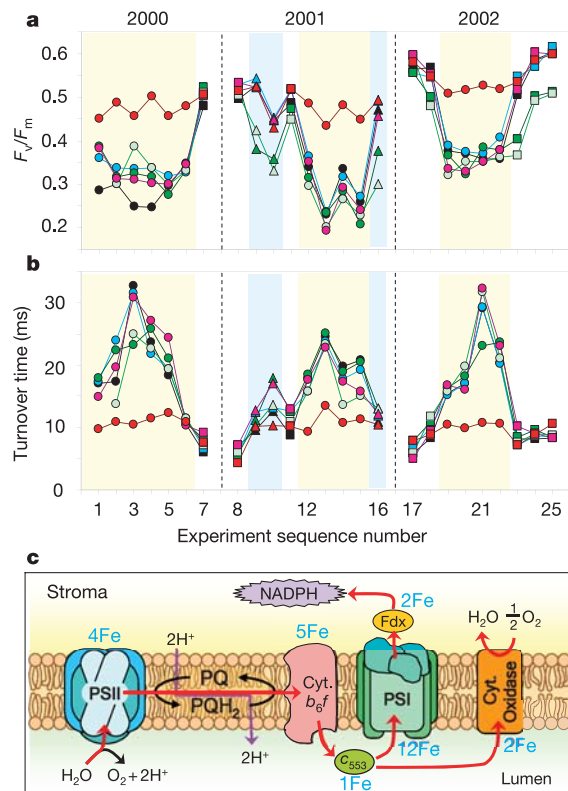


**Figure 3 | Nutrient enrichment responses in the three physiological regimes.** **a**, **b**, Initial and end-of-experiment treatment values of normalized variable fluorescence ( $F_v/F_m$ ) (**a**) and plastoquinone pool electron turnover times during the 25 enrichment experiments (stars in Fig. 1a) (**b**). Regime I is represented by squares and no background shading; regime II by triangles and blue shading, and regime III by circles and yellow shading. Black symbols and lines, zero time control; blue, end-of-experiment control; dark green,  $\text{NO}_3$ ; light green,  $\text{NH}_4$ ; pink,  $\text{PO}_4$ ; red, iron. Vertical dashed lines separate cruises (labelled at the top). Experiment sequence number ( $x$  axis) follows Fig. 1a. **c**, Primary components of a photosynthetic membrane and their iron requirements (blue text). The photosynthetic electron transport sequence is as follows: PSII to plastoquinone pool (PQ,  $\text{PQH}_2$ ) to cytochrome  $b_6/f$  to a mobile cytochrome ( $c_{553}$ ) and finally to either PSI and ferredoxin (Fdx) or a terminal cytochrome oxidase. In prokaryotes and eukaryotes, electron transport can also proceed directly from the PQ pool to terminal oxidases.

atoms required for a single complete copy of the electron transport chain (Fig. 3c)<sup>11</sup>. Iron stress significantly depletes photosynthetic components on the acceptor side of the PQ pool (cytochrome *b<sub>6</sub>f*, cytochrome oxidase, photosystem I (PSI) and ferredoxin) (Fig. 3c)<sup>12–15</sup>. These changes are responsible for the large nocturnal  $F_v/F_m$  decreases in regimes II and III.

All phytoplankton use their photosynthetic membranes for respiratory electron transport in the dark (termed ‘chlororespiration’ in eukaryotes) (Fig. 3c). Consequently, the PQ pool is generally mildly reduced at night, but under iron-stressed conditions this reduction is severe because electron transport is rate-limited by diminished cytochrome concentrations (Fig. 3c)<sup>10,12,15–18</sup>. Because the redox state of the primary electron acceptor on PSII ( $Q_A$ ) exists in equilibrium with that of the PQ pool<sup>17</sup>, severe reduction of PQ at night results in a back-transfer of electrons to  $Q_A$  that we detected as a decrease in  $F_v/F_m$ . Being a respiration-driven phenomenon, the degree of PQ pool reduction depends on the pool size of respiratory substrates. Depletion of these substrates is responsible for the modest increase in  $F_v/F_m$  each night before sunrise (Fig. 1c) and explains the observation that the nocturnal decrease in  $F_v/F_m$  cannot be artificially induced after sunrise by re-exposure to darkness<sup>17</sup> until an adequate photosynthetic pool has been rebuilt. The immediate increase in  $F_v/F_m$  at dawn results from oxidation of the PQ pool by PSI turnover (Fig. 1c), a response that can be artificially replicated at night by exposure to PSI-specific light<sup>10,17</sup>. Rapid loss of the nocturnal decrease in  $F_v/F_m$  and increased electron turnover (Fig. 3b) in regimes II and III on the addition of iron reflect an associated induction of cytochrome synthesis<sup>12,16</sup>.

The distinguishing characteristic of regime III is low dawn  $F_v/F_m$  maxima (Fig. 2a). This feature is caused by unique chlorophyll–protein complexes that are synthesized when reduced nitrogen is abundant but iron is limiting<sup>12,18–23</sup>. These complexes seem to function in a photoprotective manner, are to a large degree functionally ‘disconnected’ from PSII, and have high background fluorescence that decreases  $F_v/F_m$  (refs 11, 12, 18, 22–24). Pigment from the

complexes is immediately transferred to functional PSII antennae on iron enrichment, leading to decreased background fluorescence and increases in  $F_v/F_m$  (Fig. 3a) and PSII absorption cross-sections. This same response is regularly observed in laboratory iron-recovery experiments<sup>12,16,20,25,26</sup>, proceeds in the presence of chlorophyll synthesis inhibitors<sup>26</sup> but not protein synthesis inhibitors<sup>15</sup>, and suggests that the iron-induced complexes function as pigment reservoirs to facilitate recovery from iron stress<sup>12,20,25</sup>. In regime II, the process is simply reversed by the addition of  $NO_3$  or  $NH_4$ , which induces the synthesis of these special pigment–protein complexes that are naturally substrate limited by nitrogen availability. The occasional appearance of this ‘regime II-type’ response in regime I experiments (Fig. 3a) indicates that these northern waters, which are regulated by nitrogen and grazing, can easily be perturbed into iron-stressed conditions<sup>27</sup>.

Our two variable fluorescence diagnostics define four possible physiological regimes, three of which are present in the tropical Pacific (Fig. 4). High dawn  $F_v/F_m$  values occur in both nitrogen-limited and iron-limited systems, as long as reduced nitrogen levels are low (regimes I and II). Low dawn  $F_v/F_m$  values result when iron is limiting and elevated nitrogen levels allow the synthesis of the special pigment–protein complexes (classic HNLC conditions). Large nocturnal decreases in  $F_v/F_m$  require both iron stress and sufficient dark respiration to drive PQ pool reduction (regimes II and III). Conversely, small nocturnal decreases in  $F_v/F_m$  result when iron stress is absent or growth is too slow to cause PQ pool reduction at night. Accordingly, the fourth physiological regime, which was not found in the tropical Pacific and is defined by low dawn  $F_v/F_m$  and small nocturnal decreases (Fig. 4), is predictably observed in polar HNLC regions where iron is limiting and nitrate is replete, but growth rates are too low for significant night-time PQ pool reduction<sup>28</sup>.

The tropical Pacific basin is responsible for roughly 20% (9–14 Pg C yr<sup>-1</sup>) of global ocean productivity (see Supplementary Information) and has a prominent function in air–sea CO<sub>2</sub> exchange. Assessing constraints on productivity in this permanently stratified region is challenging because the dominant phytoplankton are naturally growing at relatively high rates (of the order of one division per day) and their standing stock changes little with nutrient enrichment<sup>4</sup>. Physiological diagnostics provide a solution to this problem and here are applied on an unprecedented scale. Special pigment–protein complexes synthesized during iron stress underlie one of our key fluorescence attributes. These structures cause an enhanced greenness in HNLC regions (that is, regime III) that is not associated with elevated photosynthesis. This effect is quantitatively related to the suppression of dawn  $F_v/F_m$  values and must be accounted for when satellite surface chlorophyll fields are used to estimate ocean productivity or to evaluate ocean-circulation–ecosystem model performance. We assessed the influence of these iron-induced structures by adjusting satellite chlorophyll fields with our variable fluorescence data from the field; we found tropical Pacific production to be 1.2–2.5 Pg C yr<sup>-1</sup> lower than for uncorrected fields (see Supplementary Information). This difference is comparable to global productivity changes during major El Niño to La Niña transitions (0.4–0.8 Pg C yr<sup>-1</sup>)<sup>7,29</sup> and underscores the importance of characterizing nutrient constraints and their physiological consequences. Our current climatological treatment unquestionably misses seasonal and interannual variations in boundaries between physiological regimes. Future evaluations will benefit if links can be established between nutritional conditions and remote sensing properties, such as Moderate Resolution Imaging Spectrometer (MODIS) solar-stimulated fluorescence.

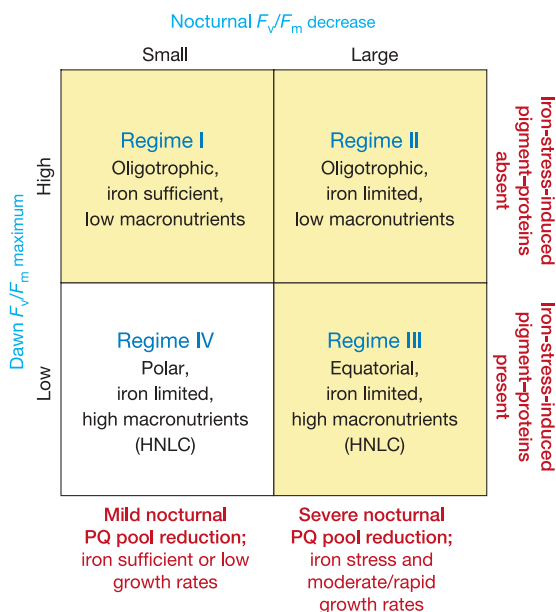


**Figure 4 | Environmental conditions corresponding to the four physiological regimes.** The regimes are distinguished by dawn normalized variable fluorescence values ( $F_v/F_m$ ) (low, less than 0.45; high, 0.45 or more) and the percentage decrease in  $F_v/F_m$  at night (small, 25% or less; large, more than 25%). Physiological and nutritional conditions responsible for the diagnostic attributes are summarized in red text to the right and at the bottom of the matrix. The three regimes observed in the tropical Pacific are identified by a yellow background.

## METHODS

The Supplementary Information contains details of all experimental methods and model calculations.

**Fluorescence.** A fast-repetition-rate fluorimeter (FRRF) was used to measure chlorophyll fluorescence characteristics of phytoplankton continuously sampled

from the surface mixed layer. The FRRf protocol involves a rapid sequence of subsaturating light flashes that cause a rise in fluorescence *in vivo* from an initial ( $F_0$ ) to a maximal ( $F_m$ ) level. This change in fluorescence ( $F_v$ ) is associated with absorbed light energy used for photosynthesis and is normalized to  $F_m$  (that is,  $F_v/F_m$ ) to account for biomass variability. Functional absorption cross-sections of PSII can also be derived from the rate of increase between  $F_0$  and  $F_m$ . Electron transport rates downstream of PSII are determined from fluorescence decay kinetics after a saturating sequence of light flashes.

Received 14 December 2005; accepted 19 July 2006.

- Coale, K. *et al.* A massive phytoplankton bloom induced by an ecosystem-scale iron fertilization experiment in the equatorial Pacific ocean. *Nature* **383**, 495–501 (1996).
- Boyd, P. W. *et al.* A mesoscale phytoplankton bloom in the polar Southern ocean stimulated by iron fertilization. *Nature* **407**, 695–702 (2000).
- Tsuda, A. *et al.* A mesoscale iron enrichment in the western Subarctic Pacific induces a large centric diatom bloom. *Science* **300**, 958–961 (2003).
- Cavender-Bares, K. K., Mann, E. L., Chisholm, S. W., Ondrusek, M. E. & Bidigare, R. R. Differential response of equatorial Pacific phytoplankton to iron fertilization. *Limnol. Oceanogr.* **44**, 237–246 (1999).
- Olson, R. J., Sosik, H. M., Chekalyuk, A. M. & Shalapyonok, A. Effects of iron enrichment on phytoplankton in the Southern ocean during late summer: active fluorescence and flow cytometric analyses. *Deep-sea Res. II* **47**, 3181–3200 (2000).
- Behrenfeld, M. J. *et al.* Biospheric primary production during an ENSO transition. *Science* **291**, 2594–2597 (2001).
- Takahashi, T. *et al.* Global sea-air CO<sub>2</sub> flux based on climatological surface ocean pCO<sub>2</sub>, and seasonal biological and temperature effects. *Deep-sea Res. II* **49**, 1601–1622 (2002).
- Chavez, F. P. *et al.* Biological and chemical response of the equatorial Pacific ocean to the 1997–98 El Niño. *Science* **286**, 2126–2131 (1999).
- Feely, R. A., Wanninkhof, R., Takahashi, T. & Tans, P. Influence of El Niño on the equatorial Pacific contribution to atmospheric CO<sub>2</sub> accumulation. *Nature* **398**, 597–601 (1999).
- Behrenfeld, M. J. & Kolber, Z. S. Widespread iron limitation of phytoplankton in the south Pacific ocean. *Science* **283**, 840–843 (1999).
- Michel, K.-P. & Pistorius, E. K. Adaptation of the photosynthetic electron transport chain in cyanobacteria to iron deficiency: The function of *IdiA* and *IsiA*. *Physiol. Plant.* **120**, 36–50 (2004).
- Vassiliev, I. R. *et al.* Effects of iron limitation on photosystem II composition and light utilization in *Dunaliella tertiolecta*. *Plant Physiol.* **109**, 963–972 (1995).
- La Roche, J., Boyd, P. W., McKay, R. M. L. & Geider, R. J. Flavodoxin as an *in situ* marker for iron stress in phytoplankton. *Nature* **382**, 802–805 (1996).
- Ivanov, A. G. *et al.* Iron stress restricts photosynthetic intersystem electron transport in *Synechococcus* sp. PCC 7942. *FEBS Lett.* **485**, 173–177 (2000).
- Sandmann, G. Consequences of iron deficiency on photosynthetic and respiratory electron transport in blue-green algae. *Photosynth. Res.* **6**, 261–271 (1985).
- Greene, R. M., Geider, R. J., Kolber, Z. & Falkowski, P. G. Iron-induced changes in light harvesting and photochemical energy conversion processes in eukaryotic marine algae. *Plant Physiol.* **100**, 565–575 (1992).
- Belkhdja, R. *et al.* Iron deficiency causes changes in chlorophyll fluorescence due to the reduction in the dark of the photosystem II acceptor side. *Photosynth. Res.* **56**, 265–276 (1998).
- Morales, F., Moise, N., Quílez, R., Abadía, A. & Moya, I. Iron deficiency interrupts energy transfer from a disconnected part of the antenna to the rest of photosystem II. *Photosynth. Res.* **70**, 207–220 (2001).
- Guikema, J. A. & Sherman, L. A. Organization and function of chlorophyll in membranes of cyanobacteria during iron starvation. *Plant Physiol.* **73**, 250–256 (1983).
- Reithman, H. C. & Sherman, L. A. Purification and characterization of an iron stress-induced chlorophyll-protein from the cyanobacterium *Anacystis nidulans* R2. *Biochim. Biophys. Acta* **935**, 141–151 (1988).
- Varsano, T., Kaftan, D. & Pick, U. Effects of iron deficiency on thylakoid membrane structure and composition in the alga *Dunaliella salina*. *J. Plant Nutr.* **26**, 2197–2210 (2003).
- Moseley, J. L. *et al.* Adaptation to Fe-deficiency requires remodeling of the photosynthetic apparatus. *EMBO J.* **21**, 6709–6720 (2002).
- Sandström, S., Ivanov, A. G., Park, Y.-I. I., Öquist, G. & Gustafsson, P. Iron stress responses in the cyanobacterium *Synechococcus* sp. PCC7942. *Physiol. Plant.* **116**, 255–263 (2002).
- Park, Y.-I. I., Sandström, S., Gustafsson, P. & Öquist, G. Expression of the *isiA* gene is essential for the survival of the cyanobacterium *Synechococcus* sp. PCC 7942 by protecting photosystem II from excess light under iron limitation. *Mol. Microbiol.* **32**, 123–129 (1999).
- Troyan, T. A., Bullerjahn, G. S. & Sherman, L. A. in *Techniques and New Developments in Photosynthesis Research* (eds Barber, J. & Malkin, R.) 601–604 (Plenum Press, New York, 1989).
- Larbi, A., Abadía, A., Morales, F. & Abadía, J. Fe resupply to Fe-deficient sugar beet plants leads to rapid changes in the violaxanthin cycle and other photosynthetic characteristics without significant *de novo* chlorophyll synthesis. *Photosynth. Res.* **79**, 59–69 (2004).
- DiTullio, G. R., Hutchins, D. A. & Bruland, K. W. Interaction of iron and major nutrients controls phytoplankton growth and species composition in the tropical North Pacific Ocean. *Limnol. Oceanogr.* **38**, 495–508 (1993).
- Boyd, P. W. & Abraham, E. R. Iron-mediated changes in phytoplankton photosynthetic competence during SOIREE. *Deep-sea Res. II* **48**, 2529–2550 (2001).
- Behrenfeld, M. J., Boss, E., Siegel, D. A. & Shea, D. M. Carbon-based ocean productivity and phytoplankton physiology from space. *Glob. Biogeochem. Cycles* **19**, GB1006, doi:10.1029/2004GB002299 (2005).

**Supplementary Information** is linked to the online version of the paper at [www.nature.com/nature](http://www.nature.com/nature).

**Acknowledgements** We thank Z. Kolber, R. O'Malley, and the crew and officers of the NOAA ships *Ka'imimoana* and *Ronald Brown*. This research was funded by the National Science Foundation, the National Aeronautics and Space Administration, and the National Oceanic and Atmospheric Administration's Tropical Atmosphere Ocean array programme.

**Author Information** Reprints and permissions information is available at [www.nature.com/reprints](http://www.nature.com/reprints). The authors declare no competing financial interests. Correspondence and requests for materials should be addressed to M.J.B. ([mjb@science.oregonstate.edu](mailto:mjb@science.oregonstate.edu)).

## Part I: Field Measurements

*Flow-through measurements:* For all field studies, phytoplankton fluorescence properties were monitored with a bench-top Fast Repetition Rate fluorometer (FRRf) (Kolber & Falkowski 1993; Falkowski & Kolber 1995). Seawater (~3 m depth sampling) from the ship's flow-through system was plumbed in darkness to a 1 cm<sup>3</sup> custom quartz flow cell and then exposed to a rapid sequence (1 ms spacing) of blue-light flashes. Fluorescence induction was recorded from an initial dark-adapted level ( $F_0$ ) to the maximum level ( $F_m$ ). Normalized variable fluorescence was calculated as:  $F_v/F_m = (F_m - F_0)/F_m$ . Functional absorption cross sections for PSII ( $\sigma_{PSII}$ ) were derived from fluorescence saturation kinetics. Turnover times for photosynthetic electron transport were determined from fluorescence decay kinetics following the saturating flash sequences. During the 1994 OliPac study (gray line in Fig. 1A of manuscript), flow-through FRRf measurements were only made during the nighttime ship transects, while discrete samples were collected during the day when the ship remained on station (1.5° latitude spacing between stations). On all other cruises, flow-through FRRf measurements were conducted continuously. All field studies were conducted under non-El Niño conditions, except during 2002 (white line in Fig. 1A) when we repeated a section of the 2000 study (purple line in Fig. 1A) to investigate the influence of El Niño conditions on nutrient stresses. Transect variable fluorescence and supporting data are available at: <http://science.oregonstate.edu/ocean.productivity> or by contacting M.J. Behrenfeld ([mjb@science.oregonstate.edu](mailto:mjb@science.oregonstate.edu)).

Interpolation of FRRf data to 2-dimensional fields of dawn  $F_v/F_m$  maxima and percent nocturnal decrease in  $F_v/F_m$  (Figures 2A,B of manuscript) was accomplished using the 'zgrid' gridding routine in the PlotPlus software package. This gridding routine applies a thin plate spline interpolation that converts irregularly spaced observations into a regular grid for contouring and display. The routine can yield a pure Laplacian solution (minimum curvature) or a pure spline solution, depending on the tension applied. For our calculations, a near-minimum curvature solution was chosen.

Downwelling photosynthetically active solar radiation (PAR) was continuously monitored at 15 s intervals with a Licor cosine-collecting light sensor (Model LI-1400). Discrete 500 ml seawater samples were also collected for determination of chlorophyll concentrations. Chlorophyll samples were gently filtered through Whatman GF/F® filters, which were then placed in glass scintillation vials with 10 ml of 90% acetone and stored in a freezer for 24 to 36 h. Chlorophyll concentration was determined from the acetone extracts using a calibrated Turner Designs® fluorometer. Chlorophyll concentrations in the tropical Pacific ranged from 0.06  $\mu\text{g L}^{-1}$  in nitrate-depleted waters to 0.36  $\mu\text{g L}^{-1}$  in nitrate-enriched (<0.1  $\mu\text{g L}^{-1}$ ) upwelling waters.

*Trace-metal sampling:* Samples for dissolved Fe determination were collected similarly to methods described in Field and Sherrell (2003). Briefly, seawater was pumped through a Teflon-lined polyethylene tube (lowered to ~10m at each station) using an air-powered polypropylene body, Teflon diaphragm deck pump, directly into a HEPA filtered laminar flow bench. Polypropylene switching valves in the flow bench allowed the flow to be directed either out to waste, for flushing the line, or through a 0.45  $\mu\text{m}$  pore size all polypropylene cartridge filter (Calyx, GE Osmonics) to collect clean filtered seawater samples. All surfaces contacting seawater were rigorously cleaned using trace-metal grade 1% HCl, followed by rinsing with deionized water (Milli-Q) and with ~60L of seawater before sampling began.

Filtered seawater samples were frozen on board ship and shipped to Rutgers University,

where they were thawed and acidified to pH ~1.8 using ultra-clean grade HCl (Fisher Optima). After sitting at this pH for at least two weeks, samples were analyzed using a modified version of the Mg(OH)<sub>2</sub> co-precipitation isotope dilution ICP-MS method (Wu and Boyle, 1998). Aliquots of 5mL were spiked with enriched <sup>57</sup>Fe (95%), allowed to equilibrate, then precipitated by raising the pH to ~10 using ultra-clean NH<sub>4</sub>OH. The resulting pellet was dissolved in 4% ultra-clean HNO<sub>3</sub> and analyzed for Fe 56/57 ratio on a ThermoFinnigan Element-1 high resolution ICP-MS set to medium resolution (M/DM~4000) to resolve oxide and hydroxide interferences. Each sample was determined with 2-8 replicate analyses. Blanks were determined by using 50uL samples of Pacific surface seawater (Fe ~0.1nM) in place of the normal 5mL sample. Blank values were typically 0.05-0.07 ±0.01-0.02 nM, depending on the run day, for a mean detection limit (3 times SD of blank) of about 0.04 nM. The same methods were used to determine iron in samples from the first iron international intercomparison exercise (Bowie et al., 2005; lab #24), during which precision was better than ±0.016nM (1 SD; n=8). Ambient iron concentrations at all experiment locations were at trace levels and ranged from 0.04 to 0.20 nM.

*Incubation Experiments:* Nutrient enrichment experiments were conducted at 25 locations during 3 cruises between 2000 and 2002 (purple, yellow, and white lines in Figure 1A of manuscript). Unfiltered, trace-metal clean seawater (see above) was dispensed into 10 L acid-washed carboys and either unaltered (i.e., control) or inoculated with 5 μM NO<sub>3</sub>, 5 μM NH<sub>4</sub>, 1 μM PO<sub>4</sub>, or 4 nM Fe. Samples were then incubated at ambient surface temperature and exposed to ~20% incident light to avoid excessive photoinhibitory light-stress. Subsamples were collected for the subsequent 21 to 36 hours and immediately analyzed with the FRRf, with triplicate measurements made for each treatment. Incubation carboys were maintained in the light or dark (depending on time of day) prior to sample collection for FRRf analysis to avoid any short-term changes in photosynthetic parameters. At the end of each incubation experiment, 500 ml samples were collected from each treatment carboy and analyzed for chlorophyll concentration following the methods described above.

*Regional Productivity Calculations:* Iron-stressed phytoplankton growing under ample reduced nitrogen concentrations (i.e., HNLC regions) synthesize special pigment-protein complexes that are functionally ‘decoupled’ from PSII, causing a rise in background fluorescence and a decrease in  $F_v/F_m$ . When abundant, these structures increase the apparent ‘greenness’ of cells and give a false impression of enhanced photosynthetic activity compared to non-HNLC conditions. If not accounted for, this phenomenon can lead to overestimates of satellite-based regional production. To quantify this effect, we implemented an iron-stress correction in two satellite productivity models: the Carbon-based Production Model (CbPM), which uses satellite-derived phytoplankton chlorophyll-to-carbon ratios to estimate growth rates (Behrenfeld et al. 2005) and the Vertically Generalized Production Model (VGPM) (Behrenfeld and Falkowski 1997), which uses sea surface temperature to estimate chlorophyll-specific photosynthetic efficiencies. For the VGPM, an exponential temperature function was employed, as this model was found to perform better in the tropical Pacific than the original VGPM polynomial function (Campbell et al. 2002).

For the 1998 to 2004 period, the standard parameterization of the CbPM gives annual tropical Pacific production values of 13.2 to 14.2 Pg C y<sup>-1</sup> (Pg = 10<sup>15</sup> g), while the VGPM variant gives smaller values ranging from 9.3 to 10.0 Pg C y<sup>-1</sup>. Our *in situ* and incubation results indicate that an  $F_v/F_m \geq 0.5$  is indicative of efficient photosystems for the tropical Pacific region. A correction for the special iron-induced pigment-protein complexes can thus be made for waters

where  $F_v/F_m$  is  $<0.5$  by adjusting the physiological variables in the two models by the factor:  $0.5/(1-F_v/F_m)$ , where  $F_v/F_m$  is from Figure 2A of the manuscript. With this correction, CbPM annual productivity decreases by 1.8 to 2.5 Pg C  $y^{-1}$  for the 1998-2004 period, which is more than twice the 0.8 Pg C  $y^{-1}$  global productivity change the CbPM assigns to the 1997-1999 El Niño to La Niña transition. Applying the same correction to the VGPM variant decreases regional annual production by 1.2 to 1.3 Pg C  $y^{-1}$ , which again significantly exceeds this model's 0.4 Pg C  $y^{-1}$  estimate for the global El Niño to La Niña productivity change. Thus, while the two models provide different absolute original and corrected values for tropical ocean productivity and global El Niño effects, our conclusions are robust across different productivity modeling approaches.

#### References:

Behrenfeld, M.J., & Falkowski, P.G. 1997. Photosynthetic rates derived from satellite-based chlorophyll concentration. *Limnol. Oceanogr.* 42:1-20

Behrenfeld, M.J., Boss, E., Siegel, D.A. & Shea, D.M. 2005. Carbon-based ocean productivity and phytoplankton physiology from space. *Global Biogeochem. Cycles*, 19, GB1006, doi:10.1029/2004GB002299

Bowie, A.R., E.P. Achterberg, P.R. Croot, H.J.W. de Baar, P. Laan, J.W. Moffett, S. Ussher, and P.J. Worsfold (2005) A community-wide intercomparison exercise for the determination of dissolved iron in seawater, *Mar. Chem.*, in press.

Campbell, J., Antoine, D., Armstrong, R., Arrigo, K., Balch, W., Barber, R., Behrenfeld, M.J., Bidigare, R., Bishop, J., Carr, M-E., Esaias, W., Falkowski, P.G., Hoepffner, N., Iverson, R., Kiefer, O., Lohrenz, S., Marra, J., Morel, A., Ryan, J., Vedernikov, V., Waters, K., Yentsch, C., & Yoder, J. 2002. Comparison of algorithms for estimating primary productivity from surface chlorophyll, temperature and irradiance. *Global Biogeochem. Cycles* 16(3): 10.1029.

Falkowski, P.G. and Kolber, Z. (1995) Variations in chlorophyll fluorescence yields in phytoplankton in the world oceans. *Aust. J. Plant Physiol.* **22**, 341-355.

Field, M.P. and R.M. Sherrell (2003) Direct determination of ultra-trace levels of metals in fresh water using desolvating micronebulization HR-ICP-MS: application to Lake Superior waters, *J. Anal. Atomic Spectros.* 18, 254-259.

Kolber, Z. and P.G. Falkowski (1993) Use of active fluorescence to estimate phytoplankton photosynthesis in situ. *Limnol. Oceanogr.* **38**, 1646-1665.

Wu, J. and E. A. Boyle, Determination of iron in seawater by high resolution isotope dilution inductively coupled plasma mass spectrometry after Mg(OH)<sub>2</sub> coprecipitation, *Anal. Chim. Acta*, 367, 183-191, 1998.

## Part II: Photoinhibition and Nocturnal Changes in the Water Column

Two striking diel features in Photosynthetic quantum efficiencies ( $F_v/F_m$ ) are the nocturnal decrease that we associate with iron limitation and the typically symmetric mid-day suppression associated with photoinhibition (Behrenfeld et al. 1998). During the 1994 OliPac study (gray line in Fig. 1A of manuscript), time-series stations were occupied at 5°S, 150°W and 16°S, 150°W (Dandonneau 1999) that permitted an investigation into how these surface features extend through the water column. What we find is that the daytime depression in  $F_v/F_m$  from photoinhibition decreases through the water column in proportion to the submarine light level, while the nocturnal decrease proceeds in parallel in all surface samples and is negligible in deeper, more light-limited phytoplankton (Fig. S1). These results are consistent with photoinhibition reflecting a light-dependent, reversible down-regulation of photosystem II (PSII) and the nocturnal decrease reflecting a nutrient-sensitive back-transfer of electrons to PSII that requires significant night photosynthate metabolism to effectively reduce the plastoquinone pool.

### References:

Dandonneau, Y. 1999. Introduction to special section: Biogeochemical conditions in the equatorial Pacific in late 1994. *J. Geophys. Res.* 104:3291-5.

Behrenfeld, M. J., Prasil, O., Kolber, Z. S., Babin, M. & Falkowski, P. G. 1998. Compensatory changes in photosystem II electron turnover rates protect photosynthesis from photoinhibition. *Photosynth. Res.* 58:259-68.

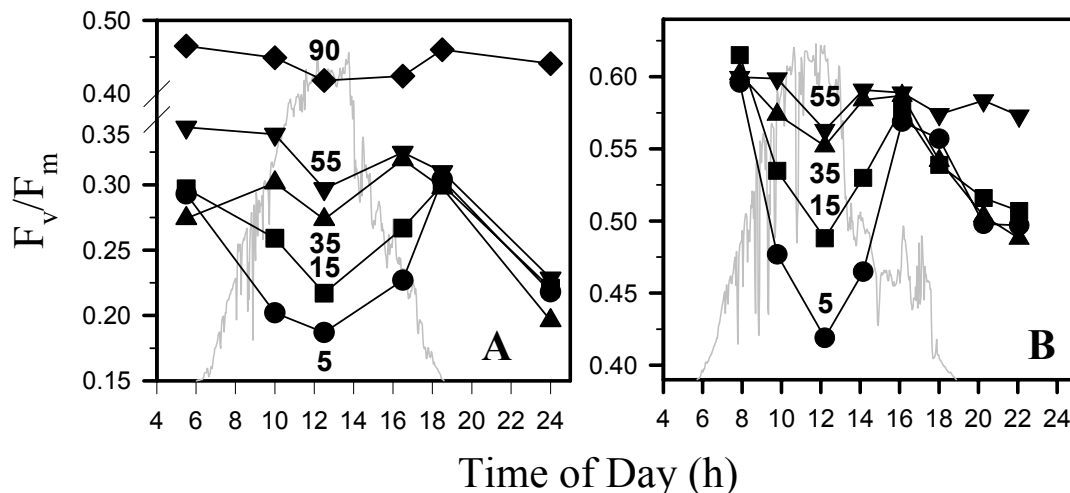


**Figure S1:** Depth-dependent diel changes in  $F_v/F_m$  observed at the two OliPac time-series stations [depths indicated next to each trace (m)]. Data in panel A are from the high-nitrate equatorial upwelling region, while data in panel B are from an extremely low nutrient, low phytoplankton biomass region. Light gray line indicates surface sunlight.

### Part III: Potential Artifacts from Blanks

Cullen and Davis (2003) describe how problems in blank determinations can have a significant influence on interpretations of oceanographic data where comparisons between absolute values are made between ocean regions. They suggest that issues with blanks can be particularly problematic in fluorescence data. Variations in blank values can result from a variety of factors; such as differences in instruments between studies, cuvette biofouling over time, or unintentional contamination of cuvettes (e.g., oils from your hands). Changes in background fluorescence from all these sources can have a non-negligible influence on derived variable fluorescence parameters if their contribution is significant relative to fluorescence yields of the sampled phytoplankton populations.

To test for significant contributions of background fluorescence to observed patterns in photosynthetic parameters in the tropical Pacific, we routinely measured blank fluorescence values using distilled water and 0.45  $\mu\text{m}$  syringe-filtered seawater each midnight before beginning the following day's continuous flow-through fluorescence record (Fig. S2). We find that our background values are more stable for freshly filtered seawater than for DI water stored in a polycarbonate vessel. In both cases, though, blank values were negligible relative to total sample fluorescence, even in highly oligotrophic waters. DI and filtered seawater blanks averaged 0.04 and 0.02 relative fluorescence units, respectively. When compared to the minimal  $F_0$  values measured during the subsequent diurnal period (i.e., yielding the maximum potential artifact), these blank values generally represented only a few percent of total fluorescence. Clearly, blanks were not a significant problem during our studies. We note, however, that great care was taken during all our field studies to minimize fouling and we concur with Cullen and Davis (2003) that attention to blanks is an important consideration for all optical measurements.

#### Reference:

Cullen, J.J., R.F. Davis. The blank can make a big difference in oceanographic measurements. *Limnol. Oceanogr. Bull.* **12**, 30 (2003)

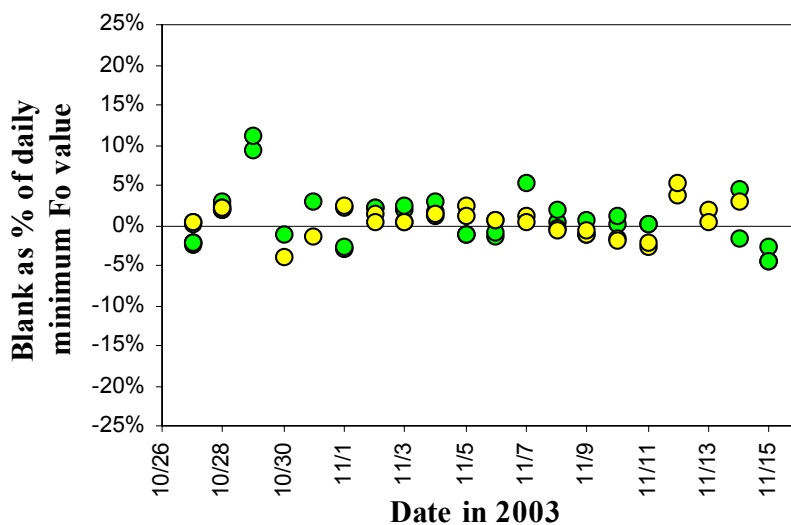


**Figure S2:** Blank values measure for freshly filtered seawater (green circles) and stored DI water (yellow circles) during the 2003 field study. Values are expressed relative to the minimum fluorescence value measured the following day with raw seawater.